

Document downloaded from:

<http://hdl.handle.net/10251/52524>

This paper must be cited as:

F. Payri; P. Olmeda; J. Martín; García Martínez, A. (2011). A complete 0D thermodynamic predictive model for direct injection diesel engines. *Applied Energy*. 88:4632-4641. doi:10.1016/j.apenergy.2011.06.005.



The final publication is available at

<http://dx.doi.org/10.1016/j.apenergy.2011.06.005>

Copyright Elsevier

1 A complete 0D thermodynamic predictive model for Direct
2 Injection Diesel engines

3 F. Payri, P. Olmeda, J. Martín*, A. García

4 *CMT-Motores Térmicos, Universidad Politécnica de Valencia, Camino de Vera s/n. 46022 Valencia,*
5 *Spain*

6 **Abstract**

7 Ideal models provide the simplest way to reproduce internal combustion engine (ICE)
8 cycles, but usually they do not represent with sufficient accuracy the actual behaviour of
9 an ICE. A suitable alternative for research and development applications is provided by
10 zero-dimensional (0D) thermodynamic models. Such models are very useful to predict the
11 instantaneous pressure and temperature in the combustion chamber, which in turn allow
12 the prediction of engine operation characteristics. However, their simplifying hypotheses
13 led in some cases to a lack of accuracy or a limited predictive capability.

14 This paper describes a 0D single-zone thermodynamic model that takes into account
15 the heat transfer to the chamber walls, the blow-by leakage, the fuel injection and engine
16 deformations, along with the instantaneous change of the gas properties. Special atten-
17 tion have been paid to the description of the specific sub-models that have been used for
18 the calculation of the energy and mass equations terms. Also the procedures followed
19 for the estimation of some mechanical and heat transfer parameters and the combustion
20 model fitting is detailed. After the fitting, the model was validated in a large amount
21 of operation points in a 4-cylinder 2-litre DI diesel engine, showing a good capability for
22 accurate predictions of the gas state during the closed cycle and engine performance.

23 *Keywords:* real cycles, thermodynamic model, heat transfer, blow-by leakage, engine
24 deformations

*Corresponding author. Tel.: +34 963877650; fax: +34 963877659
Email address: jaimardi@mot.upv.es (J. Martín)

25 **Nomenclature**

α	Crank angle	[<i>cad</i>]
c_v	Specific heat at constant volume	[<i>J/kg K</i>]
D	Cylinder bore	[<i>m</i>]
d_{comb}	Combustion duration	[<i>cad</i>]
dHR	Heat Released in a calculation step	[<i>J</i>]
EVO	Exhaust Valve Opening	
F_s	Stoichiometric fuel-air equivalence ratio	[$-$]
HRF	Cumulated Heat Release Fraction	[$-$]
γ	Adiabatic index	[$-$]
h	Specific enthalpy	[<i>J/kg</i>]
IVC	Intake Valve Closing	
<i>IMEP</i>	Indicated Mean Effective Pressure	[<i>bar</i>]
m	Mass	[<i>kg</i>]
p	In-cylinder pressure	[<i>Pa</i>]
Q	Heat transfer to the walls	[<i>J</i>], [<i>W</i>]
R	Specific gas constant	[<i>J/kg K</i>]
<i>SOC</i>	Start of Combustion	[<i>cad</i>]
<i>SOI</i>	Start of Injection	[<i>cad</i>]
T	Temperature	[<i>K</i>]
U, u	Internal energy	[<i>J</i>], [<i>J/kg</i>]
Y	Mass fraction	[$-$]

26 Subscripts

<i>a</i>	Relative to the air
<i>b</i>	Relative to the stoichiometric combustion products
<i>bb</i>	Relative to the <i>blow-by</i>
<i>c</i>	Relative to the gas mean properties in the chamber
<i>cool</i>	Relative to coolant
<i>exh</i>	Relative to exhaust conditions
<i>f</i>	Relative to the fuel
<i>f, ev</i>	Relative to the evaporated fuel
<i>f, g</i>	Relative to the gaseous fuel
<i>f, inj</i>	Relative to the liquid fuel at injection conditions
<i>in</i>	Relative to inlet conditions
<i>evap</i>	Relative to the evaporation

27 1. Introduction

28 Nowadays the main challenges in the internal combustion engines (ICE) consist on the
29 reduction of fuel consumption and emissions. With this purpose different techniques have
30 appeared to better optimize the combustion process: high pressure fuel injection systems
31 [1], multiple injections [2], high boost pressure [3], EGR [4], variable valve timing [5],
32 high swirl ratios [6], new clean fuels [7], Nevertheless, the great quantity of possible
33 configurations for each engine condition as well as the necessity of shorter engine set up
34 times, impose the use of predictive calculation models that allow to speed-up the search
35 for the optimum configuration.

36 In this framework, ideal models represent the first approach to analyze the main
37 trends of efficiency and engine power. Despite the claims by several researchers [8–10],
38 it is generally accepted [11] that, due to their intrinsic limitations, do not represent with
39 sufficient accuracy the behaviour of a current ICE.

40 To improve the ideal models performances, Bhattacharyya [12] included thermal and
41 friction losses into an equivalent friction term in order to find the maximum power output
42 varying compression ratio and cut-off ratio. On other hand, Akash [13] used a linear
43 expression to estimate the heat added to the working fluid during combustion. Chen
44 [14] conjugate previous works, i.e. he applied a linear expression for the heat transfer
45 during combustion and estimate friction losses assuming that the friction losses force was
46 a linear function of the velocity, as Angulo-Brown [15, 16] who used it for air-standard
47 Otto cycle. Al-Sharki [17] included the temperature-dependent specific heats in order to
48 improve previous works. Zhao [18] first included a new approach for determining the heat
49 leakage level as a percentage of the fuel’s chemical energy; and later on he included the
50 specific heats dependence with temperature [19]. Other improvement in ideal model is
51 carried out by [20] who used the Taylor model [21] to estimate the rate of heat loss. The
52 most recent study [22] presents a diesel engine simulation where a dual Wiebe function
53 [23] was used to model the heat release while the convective heat transfer coefficient is
54 given by the Woschni model [24]. There are similar approaches to other cycles: Otto
55 [25], Atkinson [26], Miller [27] and Dual [28].

56 In spite of the improvements performed in the ideal models by the cited authors and
57 others, they have important assumptions to solve. A suitable alternative for research
58 and development applications is provided by 0D thermodynamic models [11]. In these
59 models, the mass and energy conservation equations are solved so that the instantaneous
60 state of the gas inside the combustion chamber (pressure and temperature) is obtained.
61 However, their simplifying hypotheses led in some cases to a leak of accuracy or a limited
62 predictive capability. Their assumptions are related to the close system statement, i.e.
63 the no consideration of blow-by through the piston rings and fuel addition, the use of
64 correlations for air specific heat without considering the changes in the gas composition
65 due to the fuel injection and chemical reactions that take place during the combustion
66 process, i.e. the combustion products; and finally the consideration of a realistic heat
67 release law. All this issues are dealt with in this work.

68 The objective of the present work is to develop a 0D single-zone thermodynamic
69 model covering all the previous statements (the simulation of the rate of heat release
70 law, heat transfer and gas properties sub-models as well as blow-by leakage and the
71 fuel injection contributions to the diesel engine cycles) that have been partially covered
72 by previous researchers. 0D models do not have spatial resolution, however they can
73 consider one or more zones in the combustion chamber (mass and energy conservation
74 equations are solved for each zone). In some applications, such as emissions prediction, or
75 when the combustion details must be accounted for [29–31], it is imperative to consider
76 more than one zone in order to obtain acceptable results. However, correctly calibrated
77 and validated the proposed 0D single-zone model is suitable for the accurate calculation
78 of the pressure evolution with the purpose of predicting engine performances and fuel
79 economy or obtaining boundary conditions for specific combustion models with a high
80 computational efficiency. Starting from Intake Valve Closing (IVC) conditions (p , m and
81 T) the proposed model calculates the gas state up to the Exhaust Valve Opening (EVO)
82 thus being a predictive tool that allows rapid parametric explorations of different engine
83 operating conditions and geometric configurations.

84 2. Thermodynamic model description

85 In this section, the main hypothesis in which the thermodynamic model is based, the
86 energy and mass balances as well as a description of sub-models required to calculate
87 such balances are described.

88 2.1. Basic hypothesis

- 89 1. **Uniform pressure in the chamber is assumed.** This is normally assumed in
90 combustion calculations because both fluid and flame velocities are much smaller
91 than the sound speed [32].
- 92 2. **Three species are considered:** air, fuel vapour and stoichiometric combustion
93 products. In a DI diesel engine operating with conventional combustion, during the
94 mixing-controlled burning phase the flame is located at the stoichiometric fuel-air
95 ratio region [33] and thus this hypothesis is quite realistic.
- 96 3. **Perfect gas behaviour is assumed.** This assumption is reasonable since negli-
97 gible errors are committed as shown by Lapuerta et al. [35].

- 98 4. **Specific heats depend on temperature and gas composition.** This hypoth-
99 esis is consistent with the two previous hypotheses.
- 100 5. **Internal energy is calculated assuming mean uniform temperature in the**
101 **chamber.** This is perhaps the hardest hypothesis, as it affects the calculation of
102 the internal energy of the gas. This can be specially important for the burned
103 products at the beginning of the combustion. However, the error diminishes as
104 the combustion progresses because dilution and heat transfer tend to make the
105 temperature uniform.
- 106 6. **Heat transfer to the chamber walls is considered.** The fraction of the fuel
107 energy lost by the heat transfer to the chamber walls depends on engine size (the
108 larger the engine is the more adiabatic it is) and the operating conditions (the
109 higher the load and the engine speed are, the more adiabatic it is). For a high speed
110 DI diesel engine typical values range from 10% at full load and 4000 rpm to 30%
111 at low load and 1000 rpm. Therefore, consideration of heat transfer, depending
112 on operating conditions, is necessary in order to obtain accurate predictions of
113 indicated parameters or the thermodynamic state of the charge [36].
- 114 7. **Blow-by leakage is considered.** The blow-by mass flow is a good indicator of
115 the integrity of the piston rings and lubricant. In normal operating conditions the
116 blow-by mass flow is not important, and thus it is not usually measured. However,
117 in small DI diesel engines (0.35 l of displacement) at low engine speeds, blow-by
118 mass rates about 4% of the trapped mass have been measured; moreover, during
119 the cold start it is usual to have more than 20% [37, 38]. It is thus advisable to
120 consider this term in the mass and the energy balances, as it will be discussed
121 below.
- 122 8. **Fuel injection is considered.** Although the empirical combustion model that
123 will be described later is not based on the injection rate, the consideration of the
124 injected fuel is an important issue for both the mass and the energy balances. It has
125 been checked that the error in the energy balance (that includes the temperature
126 and gas properties errors due to the mass and composition errors) can reach a 7%
127 in the case of rich fuel-air equivalence ratio. Thus the consideration of the injected
128 mass is highly recommendable.
- 129 9. **Engine deformation is considered.** Usually, simple 0D models do not include
130 engine deformations for the instantaneous volume calculation. However, the defor-
131 mations of diesel engine, where pressure can easily reach 150 bar at the top dead
132 center, can be higher than 2% at this point. Thus a simple deformation model will
133 be used to estimate the real in-cylinder volume.

134 2.2. Energy balance

135 The energy and mass balance are solved between IVC and EVO, considering the
136 combustion chamber as an open system because of the blow-by and the fuel injection.
137 The main results are the instantaneous pressure and temperature. Accordingly to the
138 hypotheses 1 and 5, no spatial resolution of the thermodynamic properties is considered.
139 The most general expression of the First Law for an open system is:

$$\begin{aligned}
 dU_c &= -dQ + dW + h_{f,inj} dm_{f,inj} - h_c dm_{bb} \\
 &= -dQ - p dV + h_{f,inj} dm_{f,inj} - h_c dm_{bb}
 \end{aligned}
 \tag{1}$$

140 where U_c is the internal energy of the charge, Q is the heat transfer to the walls, W is
 141 the work, $h_{f,inj}$ is the specific enthalpy of the fuel at the injection conditions, $m_{f,inj}$ is
 142 the injected fuel mass, h_c is the specific enthalpy of the charge and m_{bb} is the blow-by
 143 mass.

144 As the model considers only one zone in the chamber, a single gas phase is consid-
 145 ered, and thus the injected fuel is taken into account in the mass and energy balances
 146 assuming that the evaporation takes place instantaneously. This assumption is realistic
 147 for main injections in which the time for atomization, heating and evaporation is neg-
 148 ligible, whereas this is less realistic for early pilot injections. In order to describe the
 149 process rigorously it would be necessary to follow the fuel parcel during all its evolution
 150 from the injection conditions up to the mean chamber temperature. This would require
 151 the consideration of at least two zones (liquid and gaseous phases), and thus the model
 152 complication; however, it has been checked that minor improvements in the results would
 153 be obtained.

154 Accordingly to the previous comments, Eq. (1) may be written as

$$dU_c = -dQ - p dV + h_{f,inj} \cdot dm_{f,ev} - h_c dm_{bb} \quad (2)$$

155 where the evaporated fuel mass $m_{f,ev}$ has been considered instead of injected fuel
 156 mass $m_{f,inj}$. Taking into account the hypothesis 2, the left-hand side of Eq. (2) can be
 157 expressed as:

$$\begin{aligned} dU_c &= d(m_c u_c) = d(m_a u_a + m_{f,g} u_{f,g} + m_b u_b) \\ &= m_a du_a + m_{f,g} du_{f,g} + m_b du_b + \\ &\quad + u_a dm_a + u_{f,g} dm_{f,g} + u_b dm_b \end{aligned} \quad (3)$$

158 where the subscripts c, a, f, g and b refer to chamber, air, gaseous fuel and stoichiometric
 159 burned products, respectively. The terms with $du_a, du_{f,g}$ and du_b in Eq. (3) correspond
 160 to the variation of internal sensible energy due to the change in the chamber temperature:

$$\begin{aligned} m_a du_a + m_{f,g} du_{f,g} + m_b du_b &= \\ &= m_a c_{v,a} dT + m_{f,g} c_{v,f} dT + m_b c_{v,b} dT = \\ &= m_c (Y_a c_{v,a} + Y_f c_{v,f} + Y_b c_{v,b}) dT = m_c c_{v,c} dT \end{aligned} \quad (4)$$

161 where Y represents the fuel mass fraction. In Eq. (3), the terms with $dm_a, dm_{f,g}$ and
 162 dm_b represent, respectively, the variation of the internal energy due to the composition
 163 change associated with combustion, the fuel injection and *blow-by* losses:

$$dm_a = -dm_{a,b} - Y_a dm_{bb} \quad (5)$$

$$dm_{f,g} = dm_{f,ev} - dm_{f,b} - Y_{f,g} dm_{bb} \quad (6)$$

$$dm_b = dm_{a,b} + dm_{f,b} - Y_b dm_{bb} \quad (7)$$

164 where $dm_{a,b}$ y $dm_{f,b}$ are the mass of air and fuel burned in stoichiometric conditions, so
 165 that

$$dm_{f,b} = F_s \cdot dm_{a,b} \quad (8)$$

166 Taking into account Eqs. (7) and (8), the variations of the air and fuel masses (Eqs.
 167 (5) and (6)) can be expressed in terms of the variation of the stoichiometric burned

168 mass. Substituting into Eq. (3), taking into account Eq. (4), after some algebra Eq. (1)
 169 becomes:

$$\begin{aligned} & \left[u_b - \frac{u_a + u_{f,g} F_e}{F_e + 1} \right] \cdot (dm_b + Y_b dm_{bb}) = \\ & = -m_c c_{v,c} dT - dQ - p dV + (h_{f,inj} - u_{f,g}) \cdot dm_{f,ev} - R_c T dm_{bb} \end{aligned} \quad (9)$$

170 where the first term in Eq. (9) is the heat released by combustion $-dHR$.

171 The negative sign before dHR is used for consistency with the sign criterion used for
 172 the heat transfer to the wall: positive means lost by the charge and negative supplied to
 173 the charge. In this way, dHR is positive and should be interpreted as the heat supplied
 174 to the gas as a result of combustion. If the negative sign had not been included, dHR
 175 would be the reaction energy (which would be negative since the internal energy of the
 176 combustion products is lower than that of the reactants). With this criterion, one may
 177 write:

$$dHR = m_c c_{v,c} dT + dQ + p dV - (h_{f,inj} - u_{f,g}) \cdot dm_{f,ev} + R_c T dm_{bb} \quad (10)$$

178 In Eq. (10) all the involved phenomena can be easily identified: at the left-hand
 179 side dHR is the heat released by combustion in a calculation step (the $RoHR$ can be
 180 directly obtained by dividing dHR by the angle step, $RoHR = dHR/d\alpha$), whereas the
 181 terms in the right-hand side are, respectively, the sensible internal energy of the gas, the
 182 heat transfer to the walls, the work done by the gas, the energy related to fuel injection,
 183 evaporation and heating, and the flow work associated with the *blow-by* leakage.

184 The fuel injection term can be also decomposed as follows:

$$\begin{aligned} h_{f,inj} - u_{f,g} &= h_{f,l}(T_{inj}) - u_{f,g}(T) = \\ &= [h_{f,l}(T_{inj}) - u_{f,l}(T_{inj})] - [u_{f,l}(T_{evap}) - u_{f,l}(T_{inj})] - \\ &\quad - [u_{f,g}(T_{evap}) - u_{f,l}(T_{evap})] - [u_{f,g}(T) - u_{f,g}(T_{evap})] \end{aligned} \quad (11)$$

185 where the temperature at which enthalpies and internal energies are evaluated has been
 186 indicated in brackets. The four terms in the right-hand side of Eq. (11) corresponds to:

- 187 • Specific flow work of the injected fuel
- 188 • Liquid fuel heating from the injection temperature (T_{inj}) up to the evaporation
 189 temperature (T_{evap})
- 190 • Internal energy of vaporization
- 191 • Gaseous fuel heating from the vaporization temperature up to the mean gas tem-
 192 perature (T_c).

193 To finish the description of the energy balance, it is necessary to remark that all the
 194 terms in Eq. (9) depend on different variables but all of them depends only on pressure
 195 and temperature. Thus Eq. (9) has two unknown variables and an additional equation
 196 is required to solve it: the equation of state. Accordingly with hypothesis 3 the ideal gas
 197 equation is used to close the equations system:

$$p V = m R_c T \quad (12)$$

198 Eqs. (9) and (12) are solved for each calculation step from IVC to EVO, providing
 199 instantaneous pressure and temperature as the main results. Along with them, other
 200 results are obtained of which those most important are: instantaneous mass and com-
 201 position, heat flux to the walls, and indicated parameters (pressure, work, consumption,
 202 etc.).

203 The sub-models used for the calculation of each term of Eq. (9) are described in the
 204 section 2.4.

205 2.3. Mass balance

206 The trapped mass at IVC is the addition of the induced mass of fresh air (m_a), the
 207 exhaust gas recirculation mass (m_{EGR}) and the residual gas of the previous cycle (m_{res}),
 208 to which the short-circuiting mass (m_{sc}) during valve overlap (which normally can be
 209 neglected in a 4 stroke engine) is subtracted. All of them are model inputs. The incoming
 210 masses m_a and m_{EGR} are obtained from experimental measurements, whereas m_{res} and
 211 m_{sc} are calculated with a simple filling and emptying model such as that described in
 212 [39].

213 Starting from IVC, the model calculates the instantaneous change of the mass of
 214 each species (air, fuel and stoichiometric burned products) associated with *blow-by*, fuel
 215 injection and combustion. Therefore, both instantaneous gas mass and composition can
 216 be obtained. The instaneous blow-by and fuel injected models are described in 2.4.1 and
 217 2.4.2

218 In order to calculate the thermodynamic properties of the gas (see 2.4.3), it is nec-
 219 essary to know the instantaneous gas composition [40]. Taking into account the masses
 220 involved, the mass fraction of the burned products at EVO can be expressed as:

$$\begin{aligned}
 Y_{b,EVO} &= \frac{m_f + \frac{m_f}{F_s} + (m_{EGR} + m_{res}) \cdot Y_{b,EVO} - m_{sc} \cdot Y_{b,IVC} - m_{bb} \left(\frac{Y_{b,IVC} + Y_{b,EVO}}{2} \right)}{m_a + m_f + m_{EGR} + m_{res} - m_{sc} - m_{bb}} \\
 &= \frac{1 + \frac{1}{F_s} - Y_{b,IVC} \left(\frac{m_{sc} + m_{bb}/2}{m_f} \right)}{1 + \frac{1}{F} - \frac{m_{sc} + m_{bb}/2}{m_f}} \quad (13)
 \end{aligned}$$

221 where the mean of IVC and EVO compositions has been assumed for the *blow-by* mass
 222 leakage. At IVC the composition can be expressed as:

$$\begin{aligned}
 Y_{b,IVC} &= \frac{m_{EGR} \cdot Y_{b,EVO} + m_{res} \cdot Y_{b,EVO} - m_{sc} \cdot Y_{b,IVC}}{m_a + m_{EGR} + m_{res} - m_{sc}} \\
 &= \frac{Y_{b,EVO}}{1 + \frac{m_a}{m_{EGR} + m_{res}}} \quad (14)
 \end{aligned}$$

223
 224 Substitution of Eq. (14) into Eq. (13) gives $Y_{b,EVO}$ expressed in terms of known
 225 parameters:

$$Y_{b,EVO} = \frac{1 + \frac{1}{F_s}}{1 + \frac{1}{F} - \left(\frac{m_{sc} + m_{bb}/2}{m_f} \right) \frac{1}{1 + \frac{m_{EGR} + m_{res}}{m_a}}} \quad (15)$$

226 At any intermediate instant i between IVC and EVO, the instantaneous mass fraction
 227 of burnt products can be written as a function of the heat release fraction (see section
 228 2.4.4):

$$Y_b = \frac{\left(m_f + \frac{m_f}{F_s}\right) \cdot \text{HRF} + (m_{EGR} + m_{res}) \cdot Y_{b,EVO} - m_{sc} \cdot Y_{b,IVC} - \int_{IVC}^i Y_b \cdot dm_{bb}}{m_a + \int_{IVC}^i dm_f + m_{EGR} + m_{res} - m_{sc} - \int_{IVC}^i dm_{bb}} \quad (16)$$

229 The unburnt gaseous fuel mass fraction at any intermediate instant can also be ob-
 230 tained as a function of the instantaneous heat release fraction:

$$Y_f = \frac{\int_{IVC}^i m_f - m_f \cdot \text{HRF}}{m_a + \int_{IVC}^i dm_f + m_{EGR} + m_{res} - m_{sc} - \int_{IVC}^i dm_{bb}} \quad (17)$$

231 An hence the instantaneous air mass fraction is calculated as $Y_a = 1 - Y_b - Y_f$.

232 The fuel mass injected per cycle, m_f , is obtained from experimental measurements
 233 (along with m_a and m_{EGR}). The instantaneous mass of evaporated fuel (dm_f) is obtained
 234 as described in paragraph 2.4.2.

235 2.4. Sub-models description

236 A detailed description of the sub-models used to calculate the different terms in Eq.
 237 (9) are included in the following section.

238 2.4.1. Blow-by model

239 The instantaneous mass flow of *blow-by* to the crankcase is estimated by means of
 240 the equation of an adiabatic nozzle as in [41]:

$$\dot{m}_{bb} = c_{bb} A_{ref} p \sqrt{\frac{x}{R_c T}} \quad (18)$$

241 where $x = \frac{2\gamma}{(\gamma-1)} \left[\left(\frac{p_{crk}}{p} \right)^{\frac{2}{\gamma}} - \left(\frac{p_{crk}}{p} \right)^{\frac{\gamma+1}{\gamma}} \right]$. The discharge coefficient of the nozzle, c_{bb} , was
 242 adjusted with experimental measurements so that the cumulated *blow-by* coincided with
 243 the actual flow, A_{ref} is the reference section proposed by Hohenberg [42] ($3.5 \cdot 10^{-6} D$)
 244 and p_{crk} is the crankcase pressure.

245 When the pressure ratio accomplishes:

$$\frac{p_{crk}}{p} < \left(\frac{2}{\gamma+1} \right)^{\frac{\gamma}{\gamma-1}} = \frac{p_{crit}}{p} \quad (19)$$

246 sonic conditions is reached and then the nozzle flow must be calculated considering the
 247 critical pressure instead of the crankcase pressure.

248 *2.4.2. Fuel injection model*

249 As it is justified later, the consideration of the fuel injection has an important effect
 250 on the mass balance, gas composition and energy balance and thus it must be considered
 251 to get accurate simulation results. However, as the rate of heat release (see section
 252 2.4.4) contains the main combustion information the accuracy of the injection rate shape
 253 is not a critical issue, thus a square-shaped law is assumed for the fuel injection rate.
 254 It has been checked that consideration of a more realistic injection rate produces only
 255 minor improvements in the description of the thermodynamic evolution in the combustion
 256 chamber.

257 It must be born in mind that the model is not a predictive combustion model and
 258 thus it does not account for the real effect of the injection rate on the heat release. Such
 259 an effect should be taken into account with a physical combustion model such as that
 260 proposed by Arrègle et al. [43, 44]. However, this is out of the scope of this work.

261 *2.4.3. Gas properties model*

262 The thermodynamic properties of the gas are calculated in the following way:

$$R_c = R_a \cdot Y_a + R_f \cdot Y_f + R_b \cdot Y_b \quad (20)$$

263

$$c_{v,c} = c_{v,a} \cdot Y_a + c_{v,f} \cdot Y_f + c_{v,b} \cdot Y_b \quad (21)$$

264 where subscripts c , a , f and b refer to the mean properties of the chamber, air, fuel and
 265 stoichiometric burned products, respectively. R_a , R_f and R_b are the specific constants
 266 of each species, and the specific heats at constant volume, $c_{v,a}$, $c_{v,f}$ y $c_{v,b}$ are obtained
 267 of polynomial expressions as a function of the temperature [40].

268 *2.4.4. Heat release law model*

269 The most complex process to be considered when performing the energy balance is
 270 combustion. Different proposals can be found in literature for the modelling of this
 271 phenomenon, from the simplest heat release laws proposed by Wiebe [23] or Watson
 272 [45] to the considerably more complex phenomenological models proposed by Barba [46],
 273 Hiroyasu [29] or Arrègle et al. [43, 44].

274 As stated, the objective of the proposed model is not the prediction of the physical
 275 phenomena involved in the combustion process, but the provision of accurate thermody-
 276 namic conditions in the chamber. Therefore, following the proposal of Serrano et al. [47],
 277 a simple phenomenological model with several Wiebe functions have been used in order
 278 to describe the RoHR: in operating point with pilot injection, one Wiebe function (W_1)
 279 is used to reproduce it, another three Wiebe functions (W_2 , W_3 and W_4) are always used
 280 to simulate the premixed, diffusion and late combustion phases respectively. Hence, the
 281 mathematical expression of the rate of heat release is:

$$RoHR = \sum_{i=1}^4 \left[\frac{C_i (m_i + 1)}{d_{comb,i}} \left(\frac{\alpha - SOC_i}{d_{comb,i}} \right)^{m_i} e^{\left[-C_i \left(\frac{\alpha - SOC_i}{d_{comb,i}} \right)^{(m_i+1)} \right]} \cdot \beta_i \right] \quad (22)$$

282 where α is the crank angle, $d_{comb,i}$ is the duration of the combustion phase i (pilot,
 283 premixed, diffusion or late combustion), SOC_i is the start of the combustion phase i , β_i
 284 is the proportion of the combustion phase i with respect to the whole combustion (hence
 285 its value varies between 0 and 1), C_i is the completion parameter that is traditionally

286 used to represent the combustion efficiency and m_i is the shape parameter that controls
 287 the gradient of the combustion phase i .

288 The methods follow to fit the values of $d_{comb,i}$, SOC_i , β_i and m_i will be discussed
 289 later.

290 2.4.5. Volume calculation model

291 The instantaneous volume in the cylinder is calculated as the addition of combustion
 292 chamber volume, the instantaneous displaced volume and the deformation due to pressure
 293 and inertial forces:

$$V = V_{cc} + V_{d,inst} + \Delta V_p + \Delta V_i \quad (23)$$

294 where

$$V_{cc} = \frac{V_d}{r_c - 1} \quad (24)$$

295 being V_d the total displaced volume and r_c the compression ratio. The instantaneous
 296 displaced volume $V_{d,inst}$ is calculated taking into account the engine geometry, including
 297 the piston eccentricity. The two deformation terms in Eq. (23) are based on a previous
 298 work [34]:

$$\Delta V_p = k_{def} \cdot \frac{\pi D^2}{4} \cdot \frac{p}{E_{steel}} \cdot \left(\frac{D}{D_{pp}} \right)^2 \cdot L_0 \quad (25)$$

299

$$\Delta V_i = k_{def} \cdot \frac{m_{alt} \cdot a}{E_{steel}} \cdot \left(\frac{D}{D_{pp}} \right)^2 \cdot L_0 \quad (26)$$

300 where k_{def} is a deformation coefficient that is experimentally fitted using motoring tests,
 301 as described in section 3.1 (typical values range from 1 to 3), $E_{steel} = 2.1 \cdot 10^{11} \text{ N/m}^2$ is
 302 the elasticity coefficient of the steel, D_{pp} is the piston pin diameter, m_{alt} is the mass with
 303 reciprocating motion, a is the instantaneous piston acceleration and L_0 is a characteristic
 304 length defined as:

$$L_0 = h_{pis} + L_c + \frac{S}{2} \quad (27)$$

305 where h_{pis} is the distance from the piston pin axis to the top surface of the piston, L_c is
 306 the connecting rod length and S is the stroke.

307 2.4.6. Heat transfer model

308 Concerning the heat transfer to the combustion chamber walls, in motoring tests (or
 309 during compression stroke and after the end of combustion), this process is essentially
 310 governed by convection (even though gas radiation to the walls also occurs, in those
 311 conditions this mode of heat transfer is negligible in comparison with convection [48]).
 312 While combustion is taking place, additionally to convection there is also radiation from
 313 the gas and the soot particles formed. There is no agreement with respect to the fraction
 314 of the heat transfer that is transferred by radiation: Morel and Keribar [49] obtained
 315 values ranging from 4% to 20%, whereas Heywood [11] states that this fraction can be
 316 higher than 20%. Anyway, any accurate radiative model would require the calculation
 317 of the soot formed in the spray [11, 50], which is out of the scope of this work.

318 In the present model, a variation of the expression proposed by Woschni [24, 51] is
 319 used to calculate the heat transfer coefficient. However, several efforts have been done
 320 in order to improve the original model proposed by Woschni. As described in detail in

321 two previous works [52, 53], the values of the constants in the model have been modified,
 322 and the way in which the swirl effect is considered is also different, so that more realistic
 323 predictions in direct injection Diesel engines can be achieved. Those improvements were
 324 performed by means of CFD calculations, as it is described in the cited references. The
 325 expression used for the heat transfer coefficient is:

$$h = CD^{-0.2}p^{0.8}T^{-0.53} \left[C_{W1} c_m + C_{W2} c_u + C_2 \frac{V_d T_{IVC}}{V_{IVC} p_{IVC}} (p - p_0) \right]^{0.8} \quad (28)$$

326 where $C = 0.12$ and $C_2 = 0.001$, c_m is the mean piston speed, c_u is the instantaneous
 327 tangential velocity of the gas in the chamber (see [52] for the details of the calculation),
 328 C_{W1} and C_{W2} are constants whose values are fitted (along with k_{def}) from motoring
 329 tests on a specific engine, and p_0 is the motoring pressure assuming polytropic evolution.

330 Finally, the calculation of the heat flux to the wall requires the estimation of the wall
 331 temperatures. A nodal model that calculates the mean temperature of the liner, piston
 332 and cylinder head temperatures is used [54, 55].

333 3. Experimental study: adjustment and validation

334 In the following section the adjustment process for the different models is described
 335 as well as the validation performed. The experimental measurements were carried out in
 336 a high speed direct injection diesel engine with 2.0-liter displacement. It is a currently in
 337 production engine produced by an European manufacturer. It is a four-cylinder turbo-
 338 charged engine equipped with a common rail injection system. Its main characteristics
 339 are given in Table 1. The engine was directly coupled to an electric dyno. An AVL
 340 tests system collects the mean variables (acquired at a constant sample frequency of
 341 100 Hz) necessary for controlling the engine operating point and also for the combustion
 342 diagnosis. In-cylinder pressure was measured in one of the cylinders by means of a Kistler
 343 6055B glow-plug piezoelectric transducer with a measurement range of 0-250 bar.

344 3.1. Adjustment process

345 Some of the models described in the previous section have a number of constants that
 346 have to be adjusted. In particular is necessary to set the values of the heat transfer
 347 model constant C_{W1} , C_{W2} (section 2.4.6) and the deformation model constant k_{def} (sec-
 348 tion 2.4.5); also it is necessary to fit the values of the Wiebe constants in the combustion
 349 model described in section 2.4.4. The adjustment was done using experimental measure-
 350 ments obtained through a broad parametric study of the engine, both in motoring and
 351 combustion operation conditions as described below.

352 3.1.1. Mechanical and heat transfer characterization

353 The values of the constants C_{W1} , C_{W2} and k_{def} are fitted using experimental motoring
 354 tests performed on the engine to be modeled. The adjustment method is based on
 355 the sensitivity of the thermodynamic cycle to uncertainties in motoring conditions, as
 356 Lapuerta et al. studied [56, 57]. In motoring conditions, dHR is zero and the heat
 357 transfer to the walls, dQ , can be solved in the energy balance Eq. (10), which provides
 358 an "experimental" measurement of the heat transfer based on in-cylinder pressure [57].
 359 An equivalent analysis can be done by imposing the heat transfer of the Woschni-like

360 model in Eq. (10), and then computing the error in dHR [56] (theoretically it should
 361 be zero in motoring conditions). The constant k_{def} has a characteristic effect on the
 362 thermodynamic cycle (both in terms of heat transfer to the wall and the error in dHR)
 363 and the heat transfer calculated with the Woschni-like model depends on C_{W1} , C_{W2} . It
 364 is thus possible to adjust the real value of the uncertainties so that the "experimental"
 365 heat transfer to the walls coincides with the results of the Woschni-like model and thus
 366 the error in dHR is minimised.

367 The characterization procedure is performed on a set of motoring tests with the
 368 typical range of the main Diesel engine parameters as detailed in the Table 2. The
 369 results obtained from the fitting process are $C_{W1}=1.95$, $C_{W2}=1.15$ and $k_{def}=2.64$.

370 3.1.2. Combustion model adjustment

371 The values of parameters $d_{comb,i}$, SOC_i , β_i and m_i in equation 22 are obtained by
 372 fitting the rate of heat release to experimental ones obtained with the combustion analysis
 373 tool CALMEC [34]. With the aim of providing more generality to the mathematical
 374 Wiebe combustion model, phenomenological criteria proposed by Serrano et al. [47] was
 375 followed in order to diminish the number of parameters to fit:

$$\begin{aligned}
 376 \quad & \beta_4 = 1 - \beta_1 - \beta_2 - \beta_3 \\
 377 \quad & \beta_1 > 0, \beta_2 > 0, \beta_3 > 0 \\
 378 \quad & C_i = 6.9 \quad \forall i \\
 379 \quad & SOC_1 < SOC_2 < SOC_3 \\
 380 \quad & SOC_3 = SOC_4 \\
 381 \quad & d_{comb,2} < 25 \text{ cad} \\
 382 \quad & d_{comb,4} = 130 \text{ cad} \\
 383 \quad & m_i > 0 \quad \forall i \\
 384 \quad & m_2 = 0.8
 \end{aligned}$$

385 The value of the completion parameter C_i is 6.9 so that the percentage of energy
 386 released within the combustion duration is 99.9%. This simplifications has enabled to
 387 reduce the number of adjusting parameters from 20 to 12. The rest of parameters were
 388 adjusted in 25 steady operating points (at different speed and loads) distributed in the
 389 complete engine map described in Table 3. The operating points used for the model
 390 fitting are one half of the complete experimental matrix while the other half is aimed
 391 to validate the experimental results in the following section. The Levenberg-Marquardt
 392 algorithm [58, 59] was used to perform the parameters fitting.

393 3.2. Validation of results

394 For the model validation the complementary operating points to that used for the
 395 model fitting were used. Both fitting and validation operating point are equally dis-
 396 tributed in the engine map, thus the values of the combustion model parameters in the
 397 validation operating points were interpolated from values obtained in the fitted operating
 398 points, as described in the previous section.

399 Figs. 1, 2 and 3 show the evolution of in-cylinder pressure, heat release for three
 400 different test points with a single injection (Fig. 3), a multiple injection (Fig. 2), both
 401 without EGR, and a case with EGR and two injections (Fig. 1), respectively. As can
 402 be seen, the agreement between measured and predicted heat release laws and cylinder
 403 traces is good. Ignition delay as well as premixed and diffusion combustion phases are
 404 well predicted.

405 To illustrate the general behaviour of the model, Figs. 4, 5 and 6 show the max-
406 imum in-cylinder pressure, the pressure at exhaust valve opening and indicated mean
407 effective pressure for all operating points used for both the model adjustment and model
408 validation. The maximum pressure is a good parameter to account the performance of
409 the model during the compression and the first stage of the combustion, similarly, the
410 pressure at the EVO is a good indicator of the model behaviour during the last part
411 of the combustion and expansion. Finally, the IMEP is the key parameter in all engine
412 analysis and summarises well the general accuracy of the model. As can be seen in the
413 stated figures, once the different models are adjusted using a first series of experimental
414 tests ("Model fitting" in the figure legends), it is confirmed that the predictive character
415 of the proposed tool is good ("Model validation" in the figure legends). In fact, the global
416 error is just slightly higher in the validation tests. The difference can be attributed to
417 the rate of heat release simulation; if a more accurate combustion model was used, the
418 results would improve.

419 From the practical point of view, to get accurate results in agreement with experi-
420 mental values is the key issue of a predictive model. However, it is also interesting to
421 estimate which is the contribution of each submodel to the global accuracy to identify
422 the main phenomena. With this purpose a short parametric study was performed. Its
423 objective is to analyse the sensitivity of the results to different parameters included in
424 the proposed submodels and its comparison with the effect of usual engine and operating
425 parameters (compression ratio and injection timing). Six parameters were separately
426 modified: blow-by rate, the constants of the heat transfer model (C_{W1} and C_{W2}), k_{def} ,
427 compression ratio and start of injection (SOI), also the effect of including the injection
428 rate was considered. A mean load (imep=12.5 bar) and mean engine speed (2000 rpm)
429 operating point was used for the study. For each parameter (except fuel injection) three
430 values were assumed as shown in Table 4. The effect of the injected fuel was consid-
431 ered by means of the cycle simulation with and without including this term (in both
432 the cases the rate of heat release was considered). The parameter variation ranges were
433 set according to realistic experimental and modelled results in real engines. Although it
434 is difficult to ensure the coherence of the variation of such different parameters, it was
435 checked that the result sensitivity is almost linear and thus it is easy to extrapolate if
436 different parameter range were considered. The values of C_{W1} and C_{W2} were changed
437 simultaneously; the blow-by percentage is referred to trapped mass at IVC. The effect
438 of each parameter variation on indicated pressure and maximum pressure are shown in
439 Fig. 7.

440 The global trends obtained can be easily justified as follows. If no injection fuel is
441 included the cooling effect of the evaporation is not taken into account and the specific
442 heat of the gas in the chamber will be underestimated as the specific heat of the fuel
443 is higher than those of the air and burnt products, thus higher imep and maximum
444 pressures are obtained. The effect of advancing the SOI will produce a higher pressure
445 peak and also a slightly higher imep value due to the change in the indicated diagram.
446 The increase of the heat transfer parameter leads to higher heat losses and thus both imep
447 and pressure peak diminish. If the engine deformation increases, the real compression
448 ratio will diminish and lower in-cylinder pressures will be reached, thus diminishing the
449 indicated performance of the engine. Similar conclusion can be stated if a higher blow-by
450 leakage is considered. Finally, to increase the compression ratio has the opposite effect
451 than the deformations: the higher r_c is the higher the peak pressure and imep are due

452 to the change in the instantaneous volume and indicated cycle.

453 At this point it is interesting to highly that the most influencing parameters for the
454 imep prediction are the heat transfer, the blow-by leakage and the fuel injection and all
455 of them are more important than the variation of the compression ratio or SOI. The heat
456 transfer coefficients C_{W1} and C_{W2} have an important effect on the engine performance
457 as they affect directly the heat transfer. It can be stated that if no heat transfer were
458 considered, the error in the imep prediction is similar to varying the compression ratio
459 about two points or modifying the SOI 3 cad. Concerning the blow-by, even if a lower
460 leakage of about 2% (which is completely normal in real engines) is considered, its effect
461 is higher than changing one point the compression ratio and similar to change 2 cad
462 the SOI. Similar importance has the consideration of the injected fuel. Regarding the
463 peak pressure sensitivity, the relative effect of these three parameters (fuel injection,
464 heat transfer coefficients and blow-by) is not so big as in the case of imep, anyway they
465 have a similar weight than compression ratio or SOI. In this case it is also clear that the
466 deformation has an important effect similar to blow-by or fuel injection.

467 From this comments it is easy to conclude that all the described specific submodels
468 are important to account for the corresponding phenomena, and if one or several of them
469 were not included, the accuracy of the predictions shown in Figs. 4, 5 and 6 would be
470 clearly worse.

471 4. Conclusions

472 In the proposed 0D thermodynamic model, the mass and energy conservation equa-
473 tions are solved in order to obtain the instantaneous gas state in the combustion chamber.
474 A detailed description of the sub-models used for the calculation of each term appearing
475 in the energy balance has been provided. In particular, specific sub-models to reproduce
476 the blow-by leakage, the chamber deformation due to pressure and inertial efforts, the
477 heat transfer to the chamber walls and the fuel injection have been presented.

478 Some constants in the stated sub-models needed to be adjusted and a thermodynamic-
479 based procedure has been described in short. Also the combustion heat release laws
480 needed to be estimated so that the model could have accurate predictive capability. The
481 methodology followed is based on the fitting of several Wiebe function and allowed to
482 estimate the rate of heat release in all the engine operating points.

483 Once the model adjusted, it has shown to be able to accurately reproduce the in-
484 cylinder pressure evolution in a complete matrix of combustion tests in a DI Diesel
485 engine.

486 Finally, it has been justified the necessity of including the proposed submodels for
487 accurate prediction of the engine performance and it has been quantified the error in the
488 simulation results if such submodel were not included.

489 5. Acknowledgements

490 The authors thank the Universidad Politécnic de Valencia (PAID-06-09) and Gen-
491 eralitat Valenciana (GV/2010/045) for its valuable support to this work and the referees
492 for their worthy comments.

493 **References**

- 494 [1] Wang X, Huang Z, Zhang W, Kuti OA, Nishida K. Effects of ultra-high injection pressure and
 495 micro-hole nozzle on flame structure and soot formation of impinging diesel spray. *Appl Ener*
 496 2011;88:1620-1628.
- 497 [2] Park SH, Yoon SH, Lee CS. Effects of multiple-injection strategies on overall spray behavior,
 498 combustion, and emissions reduction characteristics of biodiesel fuel. *Appl Ener* 2011;88:88-98
- 499 [3] Al-Hinti I, Samhoury M, Al-Ghandoor A, Sakhrieh A. The effect of boost pressure on the perfor-
 500 mance characteristics of a diesel engine: A neuro-fuzzy approach. *Appl Ener* 2009;86:113-121
- 501 [4] Fontana G, Galloni E. Experimental analysis of a spark-ignition engine using exhaust gas recircle
 502 at WOT operation. *Appl Energy* 2010;87:218793.
- 503 [5] Fontana G and Galloni E. Variable valve timing for fuel economy improvement in a small spark-
 504 ignition engine. *Appl Energy* 2009;86:96105.
- 505 [6] Prasad BVVSU, Sharma CS, Anand TNC, Ravikrishna RV. High swirl-inducing
 506 piston bowls in small diesel engines for emission reduction. *Appl Energy* (2011),
 507 doi:10.1016/j.apenergy.2010.12.068
- 508 [7] Kegl B. Influence of biodiesel on engine combustion and emission characteristics. *Appl Energy*
 509 2011;88:1803-1812
- 510 [8] Hou SS. Comparison of performances of air standard Atkinson and Otto cycles with heat transfer
 511 considerations. *Energ Convers Manage* 2007;48:1683-1690.
- 512 [9] Lin JC, Hou SS. Performance analysis of an air-standard Miller cycle with considerations of heat
 513 loss as a percentage of fuel's energy, friction and variable specific heats of working fluid. *Int J*
 514 *Therm Sci* 2008;47:182-191.
- 515 [10] Ge YL, Chen LG, Sun FR, Wu C. Performance of Diesel cycle with heat transfer, friction and
 516 variable specific heats of working fluid. *J Energy Inst* 2007;80:239-242.
- 517 [11] Heywood, J.B. Internal combustion engine fundamentals. New York: McGraw-Hill; 1988.
- 518 [12] Bhattacharyya S. Optimizing an irreversible Diesel cycle - Fine tuning of compression ratio and
 519 cut-off ratio. *Energ Convers Manage* 2000;41:847-854.
- 520 [13] Akash BA. Effect of heat transfer on the performance of an air-standard diesel cycle. *Int Commun*
 521 *Heat Mass* 2001;28:87-95.
- 522 [14] Chen LG, Lin JX, Luo J, Sun FR, Wu C. Friction effect on the characteristic performance of Diesel
 523 engines. *Int J Ener Res* 2002;26:965-971.
- 524 [15] Angulo-Brown F, Fernandez-Betanzos J, Diaz-Pico CA. Compression ratio of an optimized Otto-
 525 cycle model. *Eur J Phys* 1994;15:38-42.
- 526 [16] Angulo-Brown F, Rocha-Martinez JA, Navarrete-Gonzalez TD. A non-endoreversible Otto cycle
 527 model: improving power output and efficiency. *J Phys D Appl Phys* 1996;29:80-83.
- 528 [17] Al-Sarkhi A, Jaber JO, Abu-Qudais M, Probert SD. Effects of friction and temperature-dependent
 529 specific-heat of the working fluid on the performance of a Diesel-engine. *Appl Ener* 2006;83:153-165.
- 530 [18] Zhao YR, Lin BH, Zhang Y, Chen JC. Performance analysis and parametric optimum design of
 531 an irreversible Diesel heat engine. *Energ Convers Manage* 2006;47:3383-3392.
- 532 [19] Zhao YR, Chen JC. Optimum performance analysis of an irreversible Diesel heat engine affected
 533 by variable heat capacities of working fluid. *Energ Convers Manage* 2007;48:2595-2603.
- 534 [20] Al-Hinti I, Akash B, Abu-Nada E, Al-Sarkhi A. Performance analysis of air-standard Diesel cycle
 535 using an alternative irreversible heat transfer approach. *Energ Convers Manage* 2008;49:3301-3304.
- 536 [21] Taylor CF, Toong TY. Heat transfer in internal combustion engines. ASME paper 57-HT 17, 1957.
- 537 [22] Sakhrieh A, Abu-Nada E, Al-Hinti I, Al-Ghandoor A, Akash B. Computational thermodynamic
 538 analysis of compression ignition engine. *Int Commun Heat Mass* 2010;37:299-303.
- 539 [23] Wiebe I. Halbempirische formel fur die Verbrennungs-Geschwindigkeit. Verlag der akademie der
 540 Wissenschaften der Vd SSR, Moscow, 1956.
- 541 [24] Woschni G. A universally applicable equation for the instantaneous heat transfer coefficient in the
 542 internal combustion engine, SAE Paper 670931, 1967.
- 543 [25] Abu-Nada E, Akash B, Al-Hinti I, Al-Sarkhi A. Performance of a spark ignition engine under the
 544 effect of friction using a gas mixture model *J Energy Inst* 2009;82:197-205.
- 545 [26] Ebrahimi R. Effects of mean piston speed, equivalence ratio and cylinder wall temperature on
 546 performance of an Atkinson engine. *Mathematical and Computer Modelling* 2011;53:12891297.
- 547 [27] Lin JC, Hou SS. Performance analysis of an air-standard Miller cycle with considerations of heat
 548 loss as a percentage of fuel's energy, friction and variable specific heats of working fluid. *Int J*
 549 *Therm Sci* 2008;47:182-191.

- 550 [28] Ozsoysal OA. Effects of combustion efficiency on a Dual cycle. *Energ Convers Manage*
551 2009;50:2400-2406.
- 552 [29] Hiroyasu H, Kadota T, Arai M. Development and use of a spray combustion modelling to predict
553 Diesel engine efficiency and pollutants emissions (part 1). *Bulletin of the JSME* 1983;26:569-575.
- 554 [30] Egnell R. Combustion diagnostics by means of multizone heat release analysis and NO calculation.
555 SAE Paper 981424, 1998.
- 556 [31] Rakopoulos CD, Rakopoulos DC, Giacomis EG, Kyritsis DC. Validation and sensitivity analysis
557 of a two zone Diesel engine model for combustion and emissions prediction. *Energ Convers Manage*
558 2004;45:1471-1495.
- 559 [32] Williams F. *Combustion theory*. The Benjamin/Cummings Publishing Co., 1985.
- 560 [33] Faeth GM. Spray combustion phenomena. Twenty-Sixth Symposium (International) on Combustion.
561 The combustion Institute, pp. 1593-1612.
- 562 [34] Payri F, Molina S, Martín J, Armas O. Influence of measurement errors and estimated parameters
563 on combustion diagnosis. *Appl Therm Eng* 2006;26:226-236.
- 564 [35] Lapuerta M, Ballesteros R, Agudelo JR. Effect of the gas state equation on the thermodynamic
565 diagnostic of diesel combustion. *Appl Therm Eng* 2006;26:1492-1499.
- 566 [36] Rakopoulos CD, Kosmadakis GM, Pariotis EG. Critical evaluation of current heat transfer models
567 used in CFD in-cylinder engine simulations and establishment of a comprehensive wall-function
568 formulation. *Appl Ener* 2010;87:1612-1630.
- 569 [37] Payri F, Broath A, Serrano JR, Rodriguez LF, Esmoris A. A Study of the potential of intake air
570 heating in automotive DI Diesel engines. SAE Paper 2006-01-1233, 2006.
- 571 [38] Rakopoulos CD, Kosmadakis GM, Dimaratos AM, Pariotis EG. Investigating the effect of crevice
572 flow on internal combustion engines using a new simple crevice model implemented in a CFD code.
573 *Appl Ener* 2011;88:1111-1126.
- 574 [39] Payri F, Galindo J, Martín J, Arnau FJ. A simple model for predicting the trapped mass in a DI
575 Diesel engine. SAE Paper 2007-01-0494, 2007.
- 576 [40] Lapuerta M, Armas O, Hernández JJ. Diagnosis of DI Diesel combustion from in-cylinder pressure
577 signal by estimation of mean thermodynamic properties of the gas. *Appl Therm Eng* 1999;19:513-
578 529.
- 579 [41] E. Abdi Aghdam and MM Kabir. Validation of a blowby model using experimental results in
580 motoring condition with the change of compression ratio and engine speed. *Exp Therm Fluid Sci*
581 2010;34:197-209.
- 582 [42] Hohenberg G. Definition und Eigenschaften des thermodynamischen Verlustwinkels von Kolben-
583 maschinen. *Automobil-Industrie* 1976;4:15-21.
- 584 [43] Arrègle J, López JJ, García JM, Fenollosa C. Development of a zero-dimensional Diesel combustion
585 model. Part 1: analysis of the quasi-steady diffusion combustion phase. *Appl Therm Eng*
586 2003;23:1301-1317.
- 587 [44] Arrègle J, López JJ, García JM, Fenollosa C. Development of a zero-dimensional Diesel combustion
588 model. Part 1: analysis of the transient initial and final diffusion combustion phases. *Appl Therm*
589 *Eng* 2003;23:1319-1331.
- 590 [45] Watson N, Pilley AD, Marzouk M. A combustion correlation for Diesel engine simulation. SAE
591 Paper 800029, 1980.
- 592 [46] Barba C, Burkhardt C, Boulouchos K, Bargende M. A phenomenological combustion model for
593 heat release rate prediction in high-speed DI Diesel engines with common rail injection. SAE Paper
594 2001-01-2933, 2001.
- 595 [47] Serrano JR, Climent H, Guardiola C, Piqueras P. Methodology for characterisation and simulation
596 of turbocharged diesel engines combustion during transient operation. Part 2: Phenomenological
597 combustion simulation. *Appl Therm Eng* 2009;29:1501-1518.
- 598 [48] Annand WJD. Heat transfer in the cylinders of reciprocating internal combustion engines. *P I*
599 *Mech Eng* 1963;177:973-990.
- 600 [49] Morel T. and Keribar R. Heat radiation in DI Diesel engines. SAE Paper 860445, 1986.
- 601 [50] Dec J.E. A conceptual model of DI Diesel combustion based on lasersheet imaging. SAE Paper
602 970873, 1997.
- 603 [51] Woschni G. Die Berechnung der Wandverluste und der thermischen Belastung der Bauteile von
604 Dieselmotoren. *MTZ* 31/12, 1970 pp. 491-499.
- 605 [52] Payri F, Margot X, Gil A, Martín J. Computational study of the heat transfer to the walls of a
606 DI Diesel engine. SAE Paper 2005-01-0210, 2005.
- 607 [53] Payri F, Margot X, Gil A, Martín J. Prediction of heat transfer to the walls in DI Diesel engines.
608 *Proceedings of the 2nd EACC*, 2005.

- 609 [54] Torregrosa AJ, Olmeda P, Martín J, Romero C. A Tool for Predicting the Thermal Performance
610 of a Diesel Engine. *Heat Transfer Eng* 2011; doi 10.1080/01457632.2011.548639.
- 611 [55] Torregrosa AJ, Broatch A, Olmeda P, Martín J. A contribution to film coefficient estimation in
612 piston cooling galleries. *Exp Therm Fluid Sci* 2010;34:142-151.
- 613 [56] Lapuerta M, Armas O, Bermúdez V. Sensitivity of Diesel engine thermodynamic cycle calculation
614 to measurement errors and estimated parameters. *Appl Therm Eng* 2000;20:843-861.
- 615 [57] Lapuerta M, Armas O, Molina S. Study of the compression cycle of a reciprocating engine through
616 the polytropic coefficient. *Appl Therm Eng* 2003;23:313-323.
- 617 [58] Levenberg K. A method for the solution of certain non-linear problems in least squares. *The*
618 *Quarterly of Applied Mathematics* 1944;2:164-168.
- 619 [59] Marquardt D. An algorithm for least-squares estimation of nonlinear parameters. *SIAM Journal*
620 *of Applied Mathematics* 1963;11:431-441.

621 **List of figures**

622

623 Fig. 1. Experimental and simulated RoHR and pressure at 2000 rpm, 80 Nm (25% load),
624 15% EGR and 2 injections.

625 Fig. 2. Experimental and simulated RoHR and pressure at 3000 rpm, 280 Nm (100%
626 load) and 2 injections.

627 Fig. 3. Experimental and simulated RoHR and pressure at 4000 rpm, 120 Nm (50%
628 load) and single injection.

629 Fig. 4. Experimental and simulated maximum pressure.

630 Fig. 5. Experimental and simulated pressure at the exhaust valve opening.

631 Fig. 6. Experimental and simulated indicated mean effective pressure.

632 Fig. 7. Effect of the parameters on imep and maximum pressure.

633

634 **List of tables**

635

636 Table 1. Engine main characteristics.

637 Table 2. Motoring tests.

638 Table 3. Combustion tests.

639 Table 4. Parameters variation.

640

Table 1: Engine main characteristics

Displaced volume	2.0	[l]
Cylinders	4	
Bore	85	[mm]
Stroke	88	[mm]
Connecting rod length	145	[mm]
Compression ratio	17.8	
Maximum power	93	[kW]

Table 2: Motoring tests.

	1	2	3	4	Units
Speed	1000	2000	3000	4000	[rpm]
Inlet pressure	1026	1166	1129	1190	[mbar]
Inlet temperature	36	49	49	56	[°C]
Exhaust pressure	1115	1720	1620	1841	[mbar]
Exhaust temperature	32	31	32	32	[°C]

Table 3: Combustion tests.

Speed	1000-4500 (steps of 500)	[rpm]
Load	13-100	[%]
Torque	40-320 (steps of 40)	[Nm]
EGR	0-35	[%]
Rail pressure	325-1600	[bar]
Injections	1-2	[-]

Table 4: Parameters variation.
Simulation

	1	2	3
m_{bb}	0%	2%	4%
C_{W1}	0.85	1.7	2.55
C_{W2}	0.5	1	1.5
k_{def}	0	2	4
r_c	15.3	16.3	17.3
SOI	-2.4	-3.4	-4.4

Figure 1

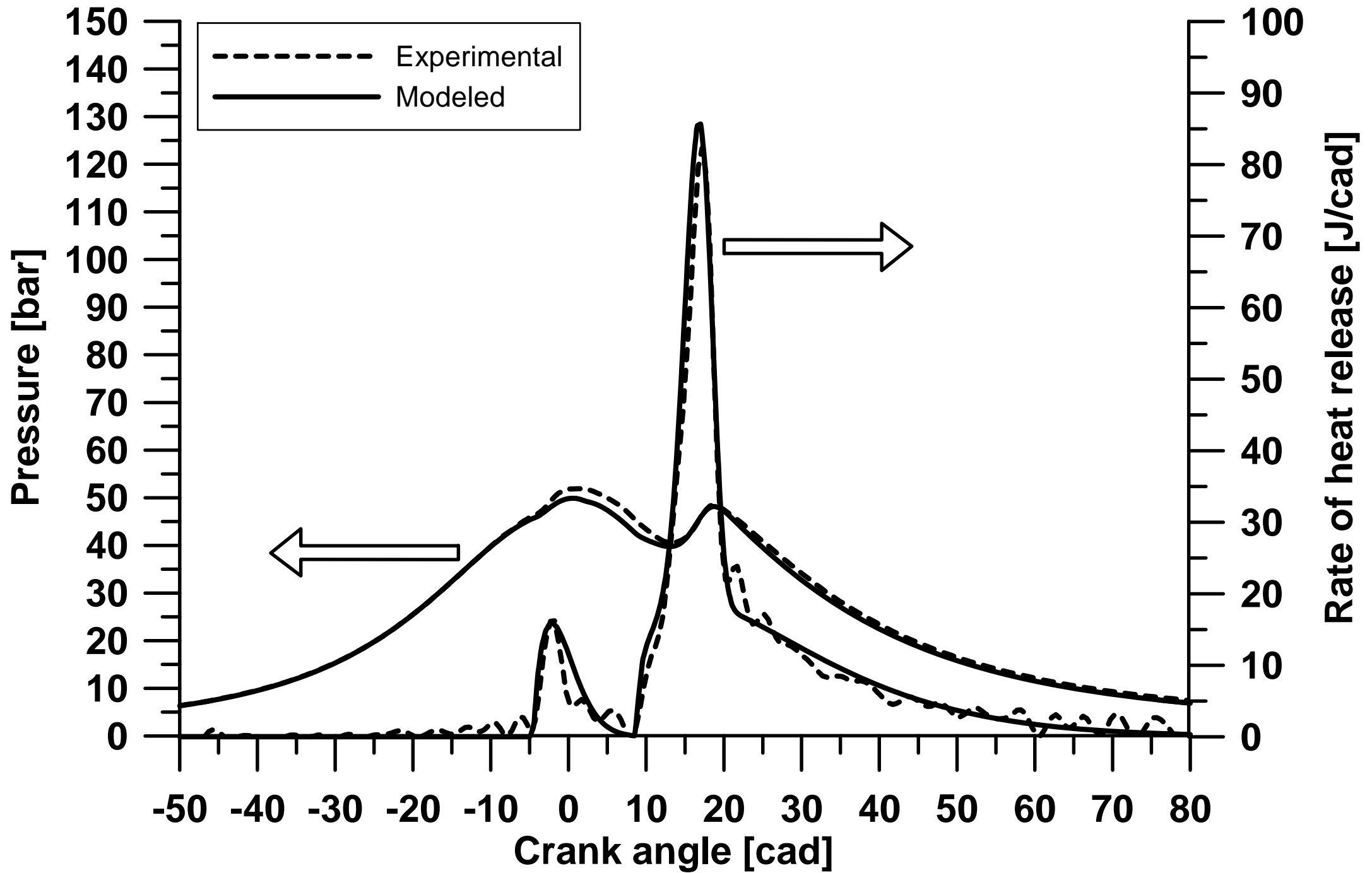


Figure 2

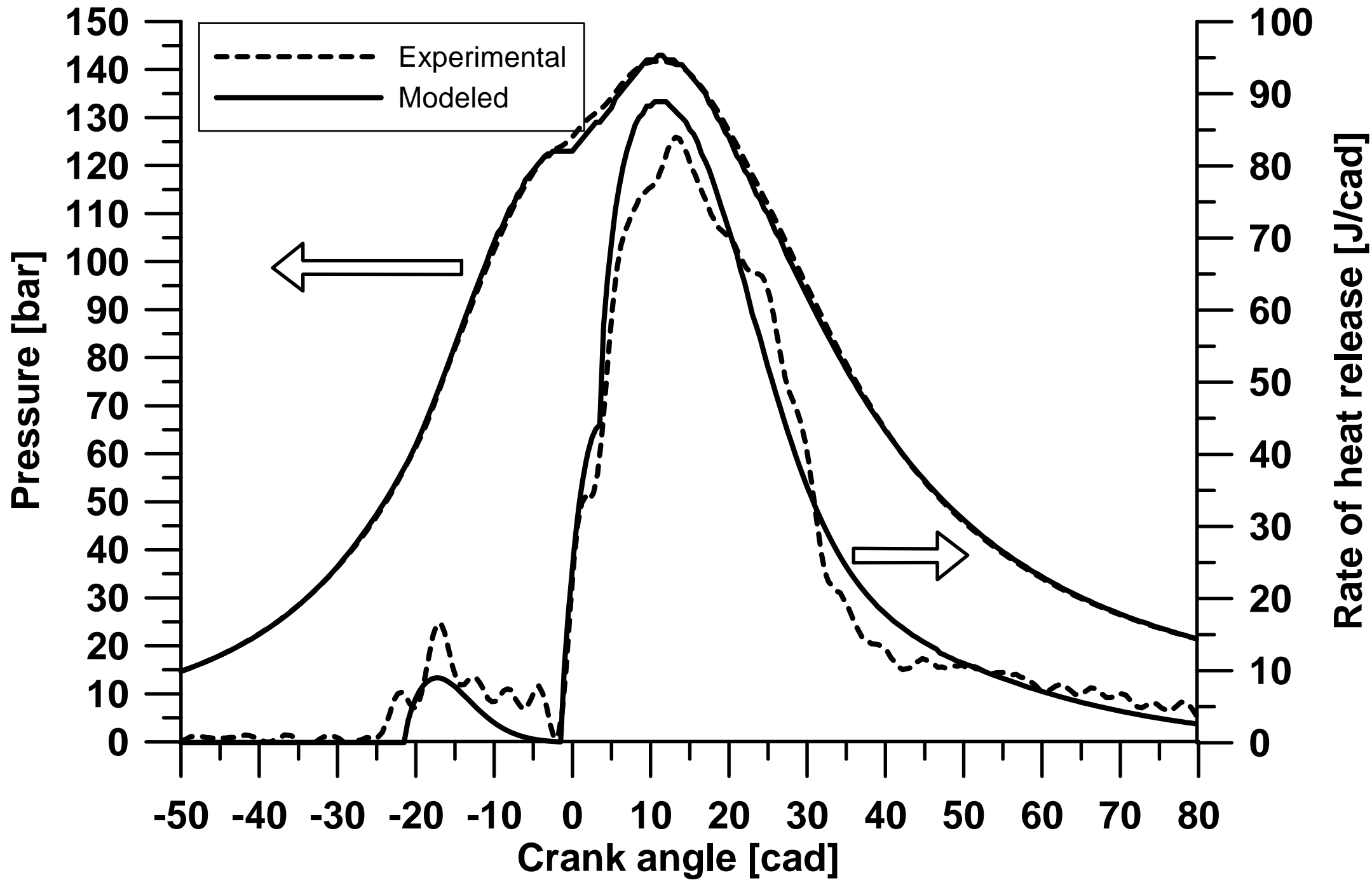


Figure 3

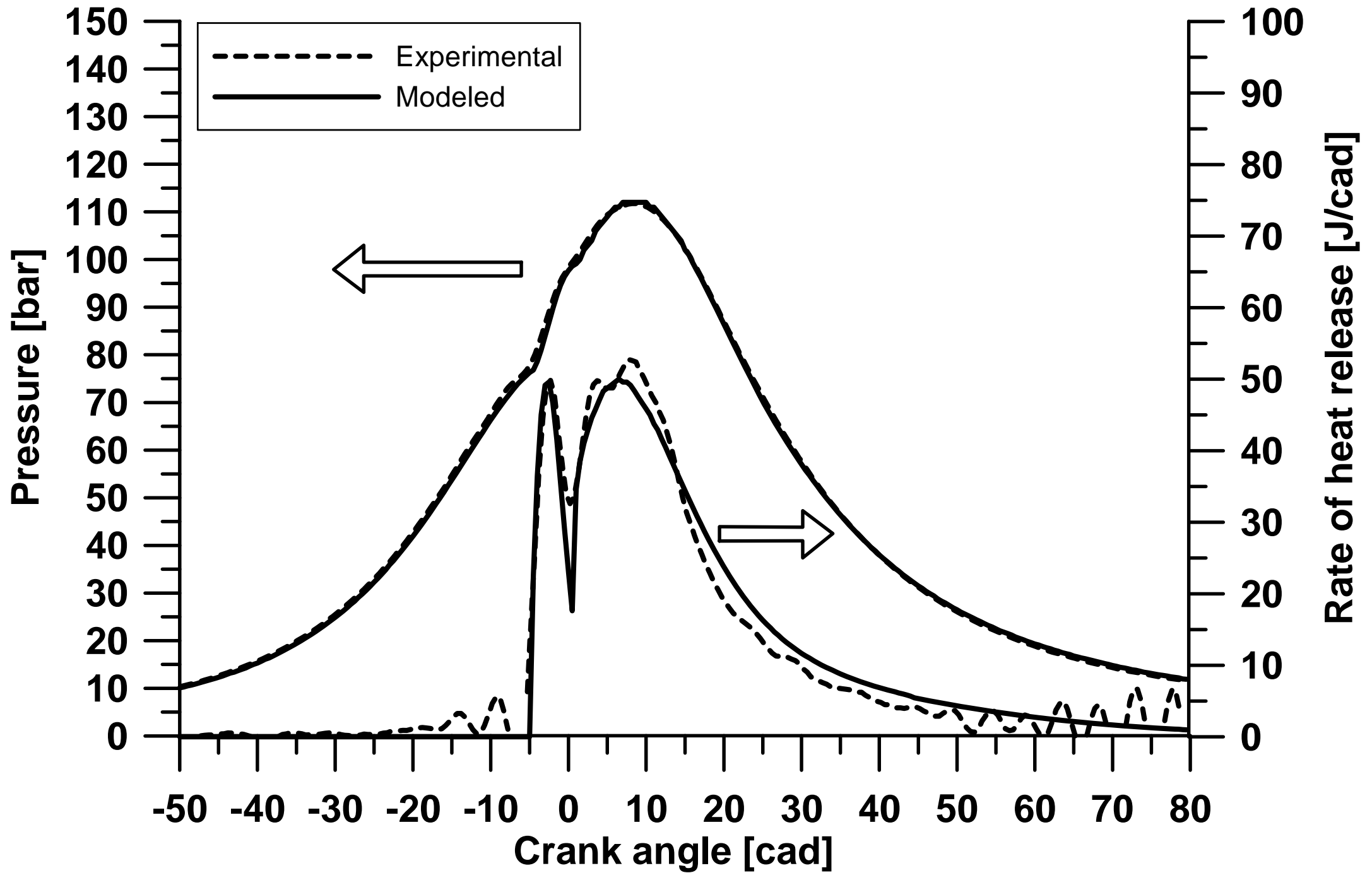


Figure 4

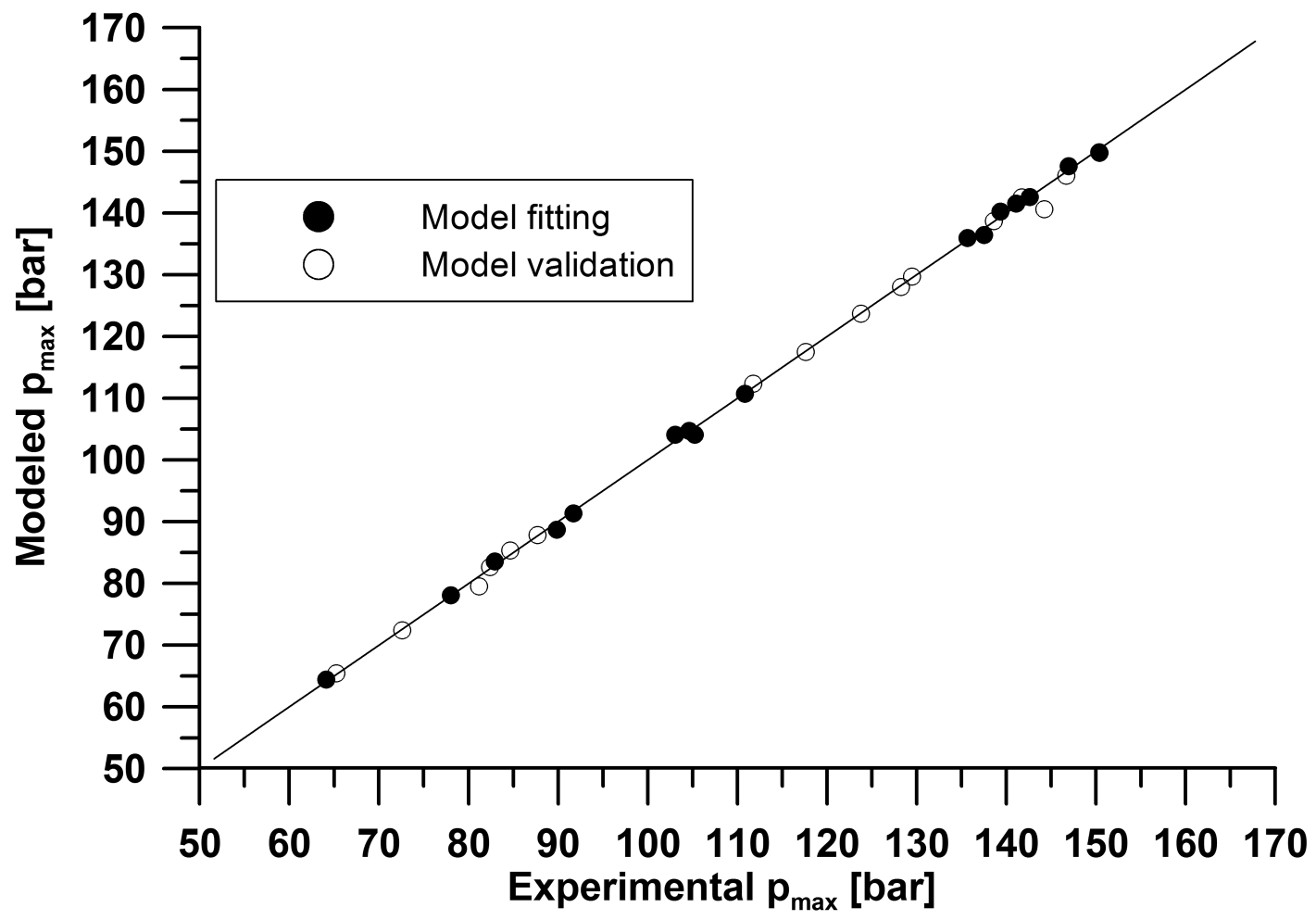


Figure 5

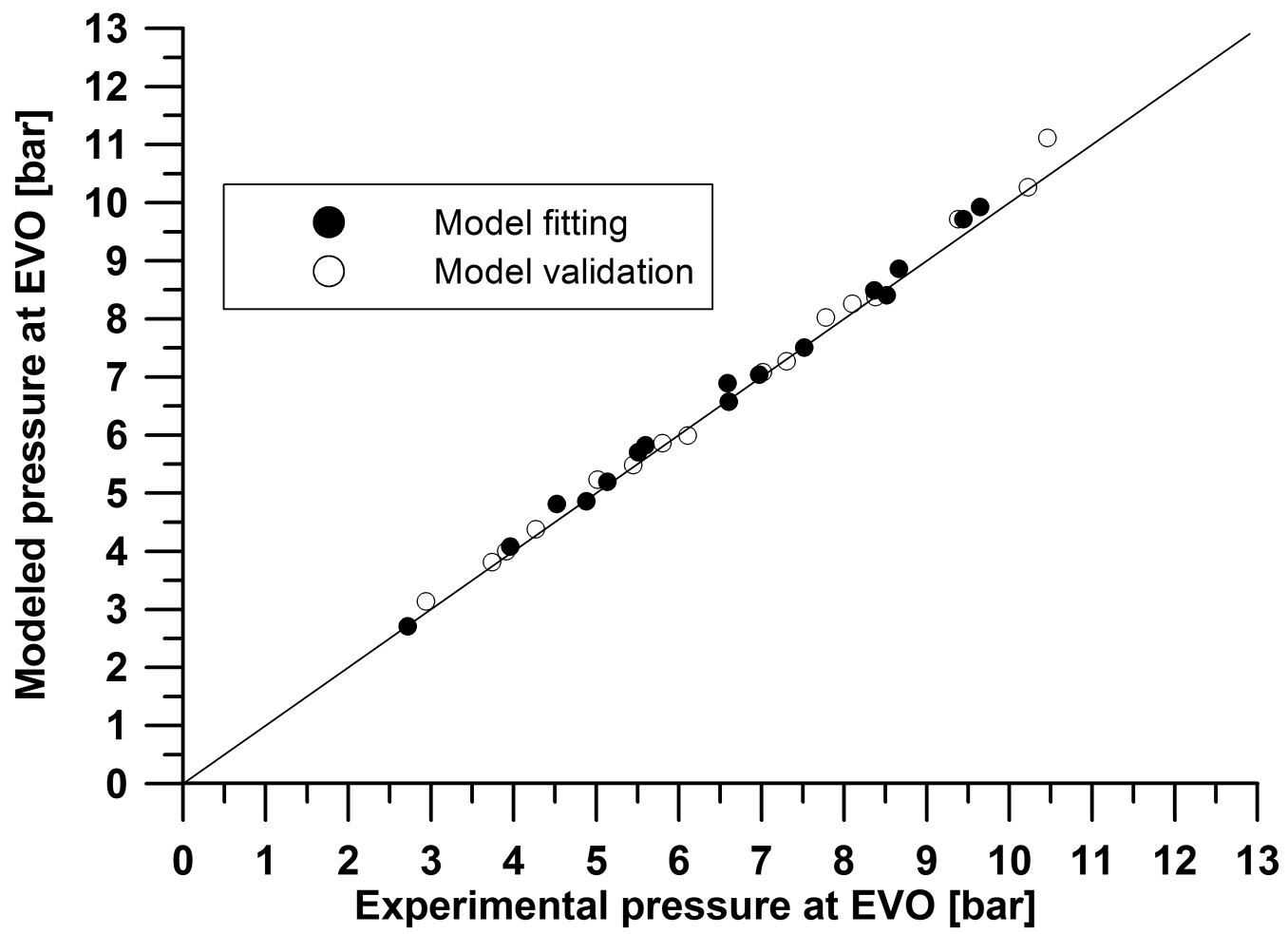


Figure 6

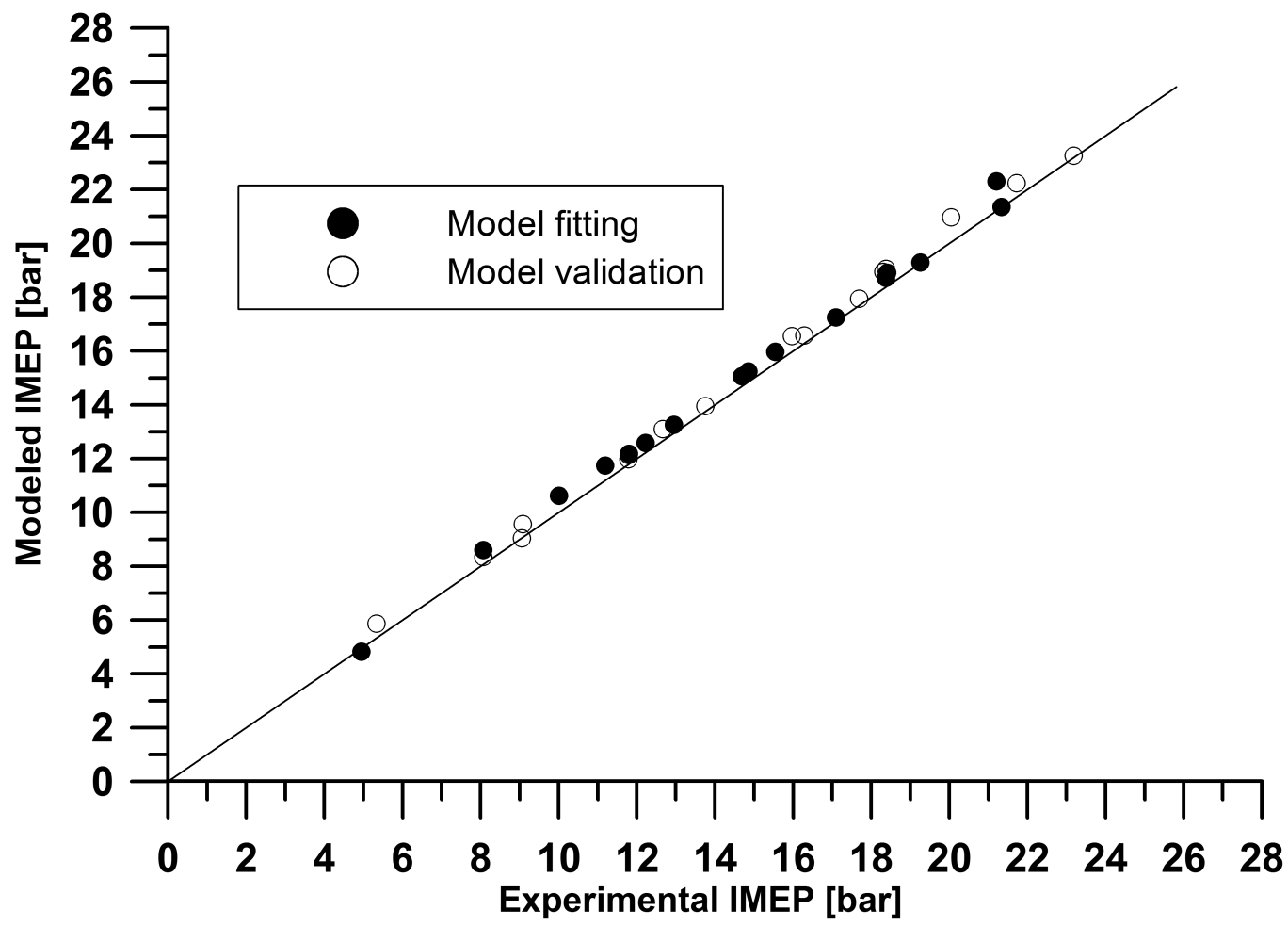
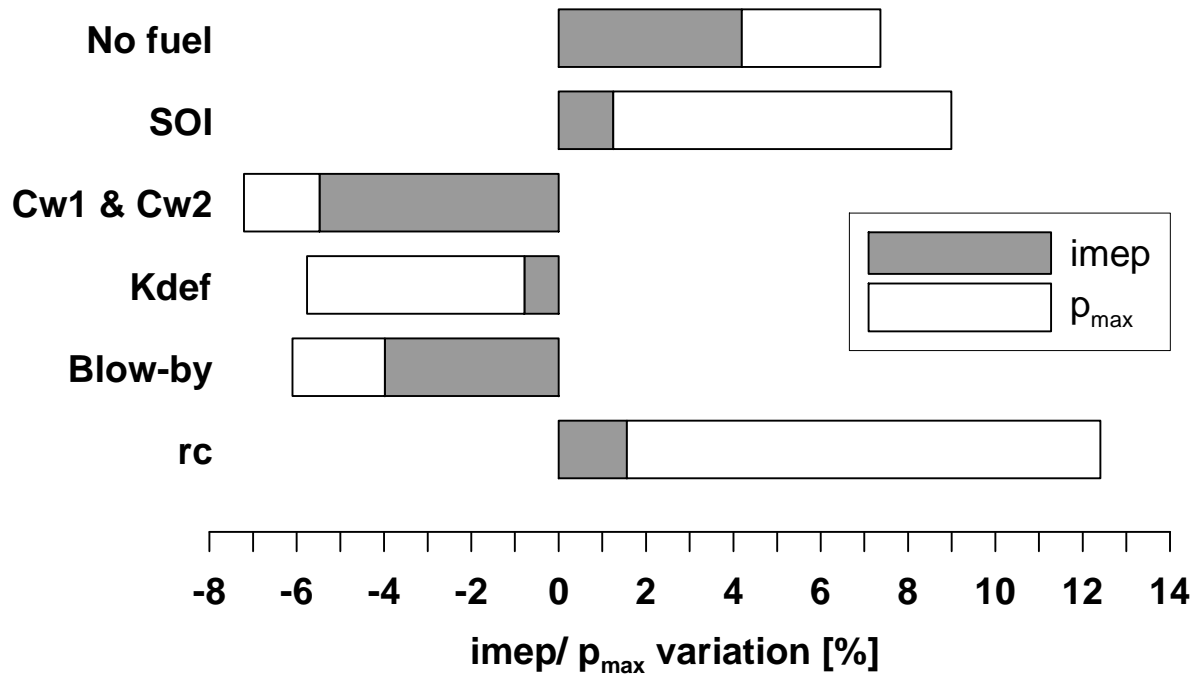


Figure 7





Valencia, February 2011

Dear Editor,

Please find enclosed the modified manuscript and figures of our article entitled “Complete 0D thermodynamic predictive model for Direct Injection Diesel engines”, by Francisco Payri, Pablo Olmeda, Jaime Martín and Antonio García to be considered for publication in the Journal Applied Energy

In the following pages we have included all the comments made by the reviewers together with our detailed answers to their points.

We hope that the modified version of the paper will be considered worth publishing in your Journal.

Yours sincerely,

Dr. Jaime Martín

jaimardi@mot.upv.es

CMT Motores Térmicos. Universidad Politécnica de Valencia

Valencia, SPAIN E-46022

Ref: APEN-D-10-01212

Title: complete 0D thermodynamic predictive model for Direct Injection Diesel engines

Authors: Francisco Payri, Pablo Olmeda, Jaime Martin and Antonio García

Reviewer #1:

First of all, we would like to thank you for your comments. They helped us to address some weak points in the initial manuscript.

In the following paragraphs we try to answer more specifically your comments:

Comments:

This paper was aimed to develop a 0D thermodynamic model that takes into account the heat transfer, the blow-by leakage, the fuel injection and engine deformations. The objective of this study seems to be rather straightforward. I recommend the authors to have a careful consideration on the points as described below.

- 1. The author claim the effect of blow-by leakage is considerable in small DI diesel engines (0.35L of displacement), but not important in normal operating conditions. However, the experimental study was carried out in a diesel engine with 2.0L of displacement. What is the point of necessity in considering the blow-by leakage?**

Extending the information stated in the section “Experimental study: adjustment and validation”, the authors would like to underline that the experimental study was carried out in a 4 cylinder high speed direct injection diesel engine with 2.0 liters of total displacement, therefore, the displacement per cylinder is 0.5 liters. Thus the considerations performed in the paper regarding with the importance of blow-by effects on performance in small DI diesel engines is completely applicable in the case of study.

On the other hand, the necessity in considering the blow-by leakage in the 0D model developed is proved with a parametrical study of sensitivity included in section 3.2. As it is shown in the new figure 7, one of the most relevant parameters to predict accurately the Imep in a HSDI is the blow-by. More information related to this topic is answered in the following question.

- 2. How about the validation of results if the effect of heat transfer, the blow-by leakage, the fuel injection and engine deformations are not individually considered in the 0D thermodynamic model? Which is the most important influence? I think the author could further discuss it to show the importance of considering these sub-models.**

Taking into account the reviewer comments a short sensitivity study has been included to illustrate the effects of the submodels in comparison with usual engine parameter and operating conditions variations (SOI and compression ratio). This study includes a new table (Table 4) and a new figure (Fig 7) and some explanations in the last paragraphs of section 3.2 Validation of results.

- 3. The legends of Fig. 1~3 only showed the experimental curve and modeled curve. However, it is not easy to distinguish which curve is related to variation of pressure or rate of heat transfer.**

According to the reviewer comment, some arrows have been included in Figs. 1-3 to make easier the differentiation between pressure traces and rate of heat release evolutions. In the authors’ opinion the information is now clear, anyway, the editor or reviewer can suggest any additional change if necessary.

- 4. The description of Fig. 4~6 was not found in manuscript.**

There was a mistake in the text at line 400. In the previous version the text stated: “To illustrate the general behavior of the model, Figs. 1, 2 and 3 show the maximum in-cylinder pressure...” and it should have stated “To illustrate the general behavior of the model, Figs. 4, 5 and 6 show the maximum in-cylinder pressure...” The correction has been done.

5. I recommend the author to replace some references with recent literature because most references in manuscript were published before year 2007.

Considering the reviewer advice the references have been updated, including several papers published after year 2007:

1. Wang X, Huang Z, Zhang W, Kuti OA, Nishida K. Effects of ultra-high injection pressure and micro-hole nozzle on flame structure and soot formation of impinging diesel spray. *Appl Ener* 2011;88:1620-1628.
2. Park SH, Yoon SH, Lee CS. Effects of multiple-injection strategies on overall spray behavior, combustion, and emissions reduction characteristics of biodiesel fuel. *Appl Ener* 2011;88:88-98.
3. Al-Hinti I, Samhouri M, Al-Ghandoor A, Sakhrieh A. The effect of boost pressure on the performance characteristics of a diesel engine: A neuro-fuzzy approach. *Appl Ener* 2009;86:113-121.
4. Fontana G, Galloni E. Experimental analysis of a spark-ignition engine using exhaust gas recirculation at WOT operation. *Appl Energy* 2010;87:2187-93.
5. Fontana G and Galloni E. Variable valve timing for fuel economy improvement in a small spark-ignition engine. *Appl Energy* 2009;86:96-105.
6. Prasad BVVSU, Sharma CS, Anand TNC, Ravikrishna RV. High swirl-inducing piston bowls in small diesel engines for emission reduction. *Appl Energy* (2011), doi:10.1016/j.apenergy.2010.12.068.
7. Kegl B. Influence of biodiesel on engine combustion and emission characteristics. *Appl Energy* 2011;88:1803-1812.
8. Al-Hinti I, Akash B, Abu-Nada E, Al-Sarkhi A. Performance analysis of air-standard Diesel cycle using an alternative irreversible heat transfer approach. *Energ Convers Manage* 2008;49:3301-3304.
9. Sakhrieh A, Abu-Nada E, Al-Hinti I, Al-Ghandoor A, Akash B. Computational thermodynamic analysis of compression ignition engine. *Int Commun Heat Mass* 2010;37:299-303.
10. Abu-Nada E, Akash B, Al-Hinti I, Al-Sarkhi A. Performance of a spark ignition engine under the effect of friction using a gas mixture model *J Energy Inst* 2009;82:197-205.
11. Ebrahimi R. Effects of mean piston speed, equivalence ratio and cylinder wall temperature on performance of an Atkinson engine. *Mathematical and Computer Modelling* 2011;53:1289-1297.
12. Lin JC, Hou SS. Performance analysis of an air-standard Miller cycle with considerations of heat loss as a percentage of fuel's energy, friction and variable specific heats of working fluid. *Int J Therm Sci* 2008;47:182-191.
13. Y. Ge, L. Chen, F. Sun, Finite-time thermodynamic modeling and analysis for an irreversible dual cycle, *Mathematical and Computer Modelling* 2009; 50: 101-109.
14. Ozsoysal OA. Effects of combustion efficiency on a Dual cycle. *Energ Convers Manage* 2009;50:2400-2406.
15. Rakopoulos CD, Kosmadakis GM, Pariotis EG. Critical evaluation of current heat transfer models used in CFD in-cylinder engine simulations and establishment of a comprehensive wall-function formulation. *Appl Ener* 2010;87:1612-1630.
16. Rakopoulos CD, Kosmadakis GM, Dimaratos AM, Pariotis EG. Investigating the effect of crevice flow on internal combustion engines using a new simple crevice model implemented in a CFD code. *Appl Ener* 2011;88:111-126.
17. E. Abdi Aghdam and MM Kabir. Validation of a blowby model using experimental results in motoring condition with the change of compression ratio and engine speed. *Exp Therm Fluid Sci* 2010;34:197-209.
18. Torregrosa AJ, Olmeda P, Martín J, Romero C. A Tool for Predicting the Thermal Performance of a Diesel Engine. *Heat Transfer Eng* 2011; doi 10.1080/01457632.2011.548639.
19. Torregrosa AJ, Broatch A, Olmeda P, Martín J. A contribution to film coefficient estimation in piston cooling galleries. *Exp Therm Fluid Sci* 2010;34:142-151.



Reviewer #5:

Thanks for your helpful comments. Your suggestions have brought a lot of light to achieve a more complete paper. Let's give you an answer to your different comments

Comments:

- 1. There seems many studies in this area as the references listed in the manuscript. I would like to author to clearly address what the major new scientific contributions of this paper compared to previous studies. I also feel author shall update the research literature to give the most recent results in this area.**

In the introduction, the following sentence has been changed accordingly to this comment:

“The objective of the present work is to develop a 0D single-zone thermodynamic model covering all the previous statements (the simulation of the rate of heat release law, heat transfer and gas properties sub-models as well as blow-by leakage and the fuel injection contributions to the diesel engine cycles) that have been partially covered by previous researchers.”

The references has been updated (see answer to question 5).

- 2. A comparison of the method in this paper to other performance evaluation of a engine shall be discussed. In particular, it needs further address how this method can be applied in the real application?**

The reviewer consideration is well addressed; however, the authors would like to underline that in sub-section 3.2 the model presented in the paper is validated versus experimental measurements derived from an in-cylinder pressure sensor. Specifically, in figures 1, 2 and 3 is possible to prove how is the temporal evolution of in-cylinder pressure and heat release for three very different engine operating conditions. Thus, as is stated in the paper, the agreement between measured and predicted cylinder traces is good and therefore, in a first stage, the applicability of the developed model in real engine conditions is shown.

Continuing with the answer and with the aim of better illustrating the general and real behavior of the model, in figures 4, 5 and 6 are shown the maximum in-cylinder pressure, the pressure at exhaust valve opening and the indicated mean effective pressure for all operating points used for both the model adjustment and model validation. Once again, considering these parameters, the accuracy of the model in real conditions is proved.